Vol. 5, No. 2, October 2024, page 280-291
JTTM: Jurnal Terapan Teknik Mesin
p ISSN 2721-5377| e ISSN 2721-7825
http://jurnal.sttmcileungsi.ac.id/index.php/jttm

Application of the VDI 2221 method in the design of an air-to-water converter device

Salvatore Johanes Rega*, Triwahyudin Rohman, Naufal Waliy Ishlah, Subekti Subekti

* Department of Mechanical Engineering, Faculty of Engineering, Mercu Buana University, Jakarta, Indonesia
Jln. Raya Meruya Selatan No.1 West Jakarta, Indonesia

*✉ salvatorjohane@gmail.com

Submitted: 05/04/2024 Revised: 26/05/2024 Accepted: 09/06/2024

Abstract: Indonesia's drought and water crisis problems have grown significantly in importance in recent years, especially in light of the country's fast population expansion, urbanization, and growing awareness of the effects of climate change. By 2040, there may be a clean water crisis in every region along Java's north coast, from Banten to Surabaya, according to projections made by the Indonesian Institute of Sciences (LIPI). The water crisis could be a major worldwide concern and will be a highly complicated issue. One approach to resolving the water shortage is to design an air-to-water converter device. The purpose of this research is to design a device that can efficiently and effectively convert air into water through condensation processes. The design will be based on the VDI 2221 Method. The rationale behind selecting the VDI 2221 Method is that it is a methodical approach to design that can help a designer generate and guide multiple design options. The primary mechanism of this apparatus is condensation, which turns air into dew points. The author utilized Solidworks 2020 to create the air-to-water conversion device. Through the stages of VDI 2221, the finest design outcomes were obtained from this design. The air-to-water converter mechanism in this design is constructed by version 2, which was chosen as the best option. Based on ASTM A36 material, theoretical calculations on the frame produced a safety factor of 1.45 and a maximum stress of 1.72414 × 108 N/m^2. Based on the turbine shaft calculation, the maximum stress of 1.07235 × 108 N/m2 and the safety factor of 2.57379 were obtained using Aluminum 6061 material.

Keywords: Air-to-water converter device; design; VDI 2221; condensation.

1. INTRODUCTION

Water is a fundamental necessity for every living being on Earth. Humans depend on water not only to meet household needs but also for production, industrial purposes, and other requirements [1]. In recent years, issues of drought and water crisis have become major concerns in Indonesia, particularly with rapid population growth, swift urbanization, and increasingly noticeable impacts of climate change [2]. The Indonesian Institute of Sciences (LIPI) estimates that the entire North Coast of Java, from Banten to Surabaya, will become urban areas and potentially experience a clean water crisis by 2040 [3].

The challenge in providing clean water lies in balancing the demand and the available supply [4]. This task is not easy, as the water demand continues to increase while its availability diminishes due to declining water quality caused by climate change and weather anomalies [5]. This has led to a water crisis that is being felt by societies around the world, including in Indonesia [6].

Humans are living beings highly dependent on water, not only for domestic household needs but also for production and industrial purposes [7]. Therefore, efforts are needed to find solutions to this issue. One solution to address this problem is through the condensation process, where air is converted into water via condensation [8]. Condensation is a phenomenon often studied in the field of heat transfer, involving the release of heat resulting in a phase change from vapor to liquid [9][10].

Based on this solution, a device capable of efficiently performing the air-to-water condensation process is required. This study aims to design a device that can convert air into water. To achieve the condensation process, components that can create the necessary temperature difference to condense water from the air are needed, which can be achieved using a thermoelectric cooler (Peltier module)

DOI 10.37373/jttm.v5i2.1126

[11]. The thermoelectric cooler is a device that can convert electrical energy into thermal energy or vice versa [12]. However, many air-to-water converter devices found today use power supplies as their source of electrical energy and require a household electrical network [13].

The use of a power supply as the main electricity source is similar to the research on the development of water-generating devices from air using Peltier modules, where this system utilizes AC input from the national power grid (PLN) to operate a DC power supply that powers the entire water-generating device. This device uses Peltier modules to cool the heatsink on the cold side. The type of Peltier module applied in this system is the TEC-12706, which operates at 12 volts and can reach currents up to 6 amperes [14]. Therefore, one of the objectives of designing this air-to-water converter device is to utilize kinetic energy converted into electrical energy through wind turbines.
The air-to-water converter device will be designed using the VDI 2221 method. The VDI 2221 design method is a design procedure issued by the Association of German Engineers [15][16]. This approach is a systematic method in the design of technical systems and technical products. The application of VDI 2221 has been widely used by Mercu Buana University students, such as in the design of waste processing equipment. Additionally, Mercu Buana University is actively developing new renewable energy sources.

2. METHOD

The stages of the process conducted in this design began with a literature review, followed by a needs analysis and a list of requirements, creating the device design, designing with the VDI 2221 method, manufacturing the device components, assembling the device, testing the device, and finally obtaining the results and conclusions from the tests of the air-to-water converter device. The process flow diagram of the air-to-water converter device design is shown in Figure 1.

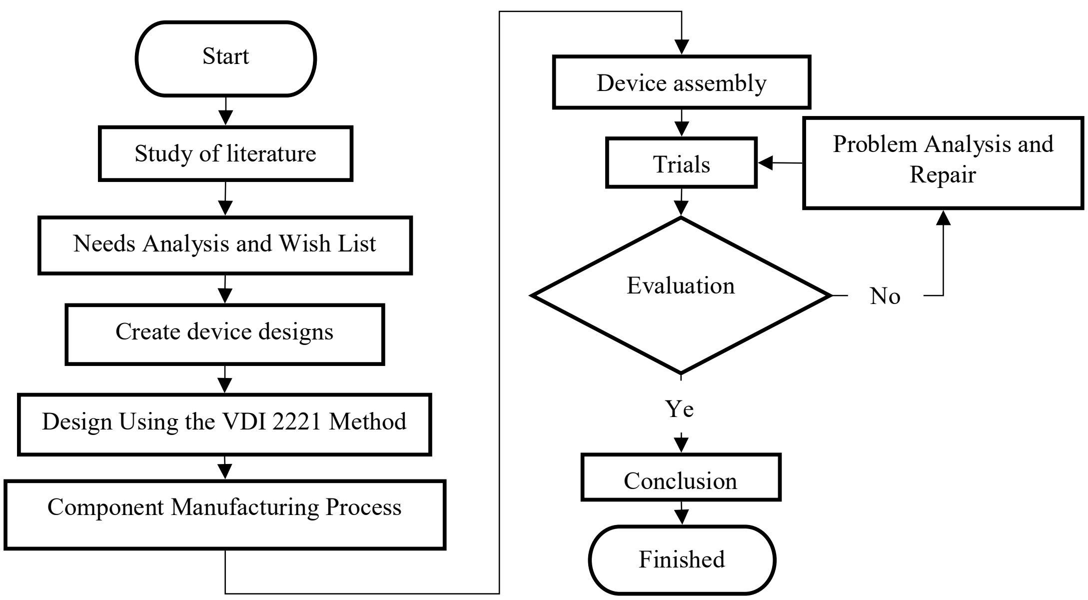

Figure 1. Design process flow diagram.

List of requirements

In designing a tool or product, a list of requirements is needed, which includes the desired or expected features or specifications of the tool or product to be designed. The function of the list of requirements is to ensure that the tool or product designed meets the needs [17]. The following are some of the requirements for designing the air-to-water converter device:

1. Has a strong frame
2. Device dimensions are not too large
3. The turbine can rotate in moderate winds
4. Easy to lift and carry
5. Does not require household electrical networks

6. Uses a battery to provide power
7. Easy to assemble and disassemble
8. Safe in operation
9. Materials are easy to find
10. Affordable material cost
11. Easy to operate
12. Corrosion-resistant turbine shaft
13. The turbine blades are not too large
14. Produces water within 1 hour
15. Space-efficient
16. Requires minimal maintenance

The above order is the list of requirements or specifications that will be arranged according to their respective parameters. Each specification will be divided into two categories: demands (D) and wishes (W), as shown in Table 1.

Table 1. List of specifications.

Parameter	D/W	Specification
Geometry	D	Dimensions are not too large
	D	Turbine blades are not too large
Material	D	Materials are easy to find
	D	Corrosion-resistant turbine shaft
	D	Has a strong frame
Function	D	The turbine can rotate in moderate winds
	D	Produces water within 1 hour
Ergonomics	D	Easy to operate
	W	Easy to assemble and disassemble
	D	Easy to lift and carry
	D	Space-efficient
Energy	D	Does not require household electrical networks
	D	Uses a battery to provide power
Cost	W	Affordable material cost
Safety	D	Safe in operation
	D	No sharp corners
Maintenance	W	Requires minimal maintenance

Abstraction

Abstraction is the process of simplifying the existing list of requirements to make it more focused. The abstraction process is carried out by eliminating wishes and considering factors directly related to the main function and primary constraints.

Abstraction 1

In Abstraction, Table 1, all wishes from the list of requirements are removed, and one of the demands from the specification table is selected.

Table 2. Abstraction 1.

Parameter	D/W	Specification
Geometry	D	Dimensions are not too large
Material	D	Materials are easy to find
Function	D	Produces water within 1 hour
Ergonomics	D	Easy to assemble and disassemble
Energy	D	Does not require household electrical networks

Parameter	D/W	Specification
Cost	D	Affordable material cost
Safety	D	Safe in operation
Maintenance	D	Requires minimal maintenance

Table 2 explains Abstraction 1, which is arranged to simplify or focus on priorities by eliminating less important wishes and selecting one crucial or necessary demand from the list of specifications. Abstraction 1 is performed to formulate or determine a more directed and effective action or decision.

Abstraction 2.

In Abstraction Table 2, factors directly related to the main function and primary constraints are considered.

Table 3. Abstraction 2.

Parameter	D/W	Specification
Function	D	Produces water within 1 hour
Energy	D	Does not require household electrical networks
Safety	D	Safe in operation

Table 3 explains Abstraction 2, which is designed to conduct a more focused analysis of factors directly related to the main function of the air-to-water converter device. Abstraction 2 also considers constraints in the development or operation of the air-to-water converter device.

Functional Structure

After the device specifications have been obtained, the next step is to create the function structure. The function structure is a framework that defines the performance of the device described in the flow of inputs and outputs, as shown in Figure 2.

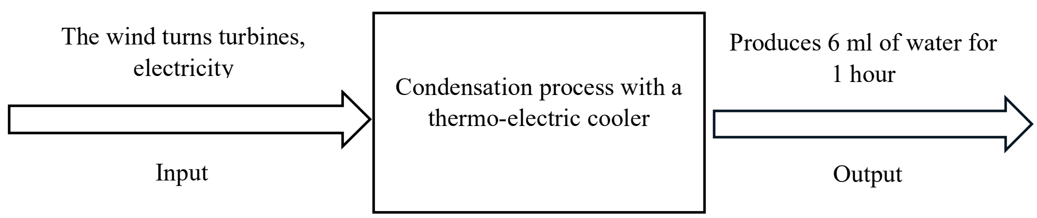

Figure 2. Overall function structure.

3. RESULTS AND DISCUSSION

Principle of Sub-Function Solutions

Once the function structure is identified, the next step is to design solutions for each sub-function by selecting various variants. The principle of solutions for sub-functions can be seen in Table 4.

Table 4. Principle of Sub-Function Solutions.

No	Sub-Function	A	B	C
1.	**Frame**	Wood	ASTM A36	SS 304
2.	**Shaft**	AISI 4140	Aluminum 6061	AISI 410
3.	**Turbine Blades**	Galvanized Plate	Plastic	Zinc Aluminum Plate
4.	**Generator**	12 V Generator	48 V Generator	24 V Generator

5.	**Thermoelectric Cooler**	TEC 12706	TEC 12705	TEC 127012
6.	**Outer Heatsink**	110 mm × 100 mm	200 mm × 100 mm	150 mm × 80 mm
7.	**Inner Heatsink**	40 mm × 40 mm	80 × 80 mm	50mm × 50mm
8.	**Cooling Fan**	12 V DC Cooling Fan (120 mm × 120 mm)	12 V DC blower	12 V DC Cooling Fan (120 mm × 120 mm)
9.	**Cooling Box**	Acrylic	Polycarbonate	Styrofoam
10.	**Turbine Pulley**	Aluminum	Nylon	Polycarbonate
11.	**Generator Pulley**	Aluminum	Nylon	Polycarbonate
12.	**Power Storage**	Accumulator	Power Supply	Battery
13.	**Controller**	Solar charge Controller	Wind Turbine Charge Controller	
14.	**Funnel**	Iron Funnel	Plastic Funnel	
15.	**Bearing**	SKF 6305	UCF 205	UCP 205
16.	**Drive System**	O-ring Rubber	Serpentine Belt	V-belt

V1 V2 V3

Based on the results of the specification checks above, several combinations or variants are obtained, namely:

Variant 1 = 1A, 2A, 3B, 4A, 5C, 6C, 7C, 8B, 9C, 10A, 11B, 12C, 13A, 14B, 15A, 16A
Variant 2 = 1B, 2B, 3A, 4A, 5A, 6A, 7A, 8A, 9A, 10A, 11B, 12A, 13A, 14B, 15B, 16A
Variant 3 = 1C, 2C, 3C, 4A, 5A, 6A, 7A, 8A, 9A, 10A, 11A, 12A, 13A, 14B, 15C, 16C

3.1. Variant Selection

In the variant selection process, a selection chart will be used to facilitate the selection. The selection chart is a visual tool that can assist in choosing options or alternatives based on certain criteria. The selection chart will be shown in Table 5.

Table 5. Selection Chart.

Selection Chart	
Criteria for Selection	Decision Indicator

(+) Yes	(+) Desired Solution
(-) No	(-) Expected Solution
(?) Insufficient information	(?) Gather Information
(!) Check Specifications	(!) Check Specifications

	Alignment with Overall Function	Alignment with List of Requirements	This can be realized in Principle	Within Production Cost Constraints	Adequate Conceptual Knowledge	Meets Designer's Wishes	Meets Safety Requirements	Explanation	SV
V1	+	-	+	+	+	-	-	Not Suitable	-
V2	+	+	+	+	+	+	+	Suitable	+
V3	+	+	-	-	-	-	+	Not Suitable	-

Based on the selection chart table above, the variant that best meets the design concept is variant 2. Therefore, the design of the air-to-water converter device will be carried out according to variant 2. In variant 2: the frame uses ASTM A36 material, the shaft uses aluminum 6061 material, the turbine blades use galvanized plate material, a 12-volt generator is used, the thermoelectric type used is 12706, the outer heatsink uses a size of 110 mm × 100 mm, the inner heatsink uses a size of 40 mm × 40 mm, a 12 V DC cooling fan (120 mm × 120 mm) is used, the cooling box uses acrylic material, turbine pulleys use aluminum material, generator pulleys use nylon material, power storage uses an accumulator, a solar charge controller (SCC) is used, a plastic funnel is used, bearings with type UCF 205 are used, and the drive system used is an o-ring rubber system.

3.2. Selected Design

Figure 3. Design of selected device with variant 2.

Figure 3 displays the design of the air-to-water converter device selected according to variant 2. In the design process, the designer utilized Solidworks 2020 software, enabling the creation of detailed and realistic 3D models.

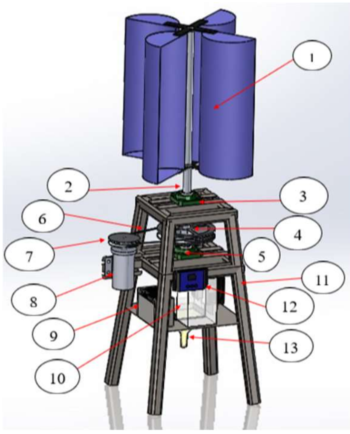

Figure 4. Component assembly.

Figure 4 illustrates the list of components within the air-to-water converter device. Each component, indicated by a number, will be detailed according to its specifications. The list and specifications of the components of the air-to-water converter device are as follows:

a. Turbine Blades: Utilizes galvanized plate material.
b. Shaft: Utilizes Aluminum 6061 material.
c. Bearing 1: Utilizes pillow block bearing with type UCF 205.
d. Turbine Pulley: Utilizes aluminum material and measures 8 inches.
e. Bearing 2: Utilizes pillow block bearing with type UCF 205.
f. O-ring Rubber: Measures 200 cm with a thickness of 3.5 mm.
g. Generator Pulley: Utilizes nylon material with a size of 59 mm.
h. Generator: Utilizes a permanent magnet generator 50-100W, with an output voltage of 12 V at a rotational speed of 150-200 rpm.
i. Accumulator: Utilizes a 12 V 7 AH accumulator.
j. Cooling Box Set with acrylic material and its contents (Thermoelectric cooler 12706, Inner heatsink measuring 40 mm × 40 mm, Outer heatsink measuring 110 mm × 100 mm, Cooling fan utilizing DC 12 V measuring 120 mm × 120 mm).
k. Frame: Utilizes ASTM 36 material.
l. Controller: Utilizes a solar charge controller.
m. Funnel: Utilizes plastic material.


Figure 5. Completed air-to-water converter device.

Figure 5 displays the air-to-water converter device that has been designed based on variant 2. This device functions successfully and can produce 6 ml of water within 1 hour of testing.

Theoretical calculation results

In the frame section of the air-to-water converter device utilizing ASTM A36 material, the frame is subjected to a load of 24 N and placed on the support rod located in the middle of the frame, as shown in Figure 6.

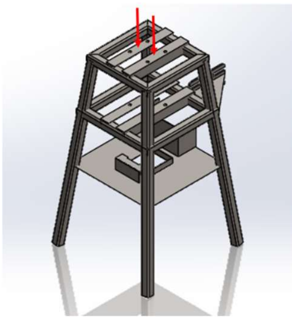

Figure 6. Loading situation of the middle support rod.

Figure 6 illustrates the loading situation on the middle support rod within the frame structure. Analyzing this loading is crucial to ensure the overall strength, stability, and safety of the frame.

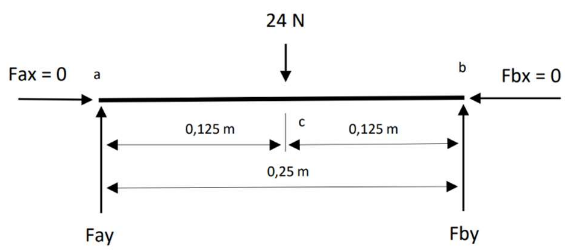

Figure 7. Free body diagram of the middle support rod.

Reaction Forces

To determine the reaction forces on the middle support rod of the frame, we can utilize equation (1):

$$\sum \mathrm{Fy} = 0 \quad (1)$$

$$+\,\mathrm{Fby}\,(0.25) - 24\,(0.125) = 0 \qquad -\,\mathrm{Fay}\,(0.25) + 24\,(0.125) = 0$$

$$0.25\,\mathrm{Fby} = 3 \qquad 0.25\,\mathrm{Fby} = -\,3$$

$$\mathrm{Fby} = 12\ \mathrm{N} \qquad \mathrm{Fay} = 12\ \mathrm{N}$$

Shear Force and Bending Moment

To determine the shear force and bending moment on the middle support rod of the frame, we can use equation (2).

$$0 \leq \mathrm{X} < 0.125 \quad (2)$$

$$\sum \mathrm{Fy} = 0 \qquad \sum \mathrm{M} = 0$$

$$12\ \mathrm{N} - \mathrm{V} = 0 \qquad 12\,\mathrm{X} + \mathrm{M} = 0$$

$$-\mathrm{V} = 12\ \mathrm{N} \qquad \mathrm{M} = 12\ \mathrm{N}$$

$$\mathrm{V} = 12\ \mathrm{N} \qquad \mathrm{M} = 12\,\mathrm{X}\ \mathrm{N.m}$$

$$\mathrm{X} = 0\ \mathrm{M} = 0\ \mathrm{N.m}$$

$X = 0.125\ M = 12\ (0.125) = 1.5\ N.m$

$\sum Fy = 0$

$12\ N - 24\ N - V = 0$

$-12 - V = 0$

$-V = 12\ N$

$V = -12\ N$

$\sum M = 0$

$M + 24\ (X - 0.25) - 12\ (X) = 0$

$M + 24\ X - 3 - 12\ X = 0$

$M + 12\ X - 3 = 0$

$M = (3 - 12\ X)\ N.m$

$X = 0.125\ M = 3 - 12\ (0.125) = 1.5\ N.m$

$X = 0.25\ M = 3 - 12\ (0.25) = 0$

After obtaining the results of the shear force and bending moment calculations on the middle support rod of the frame, shear force and bending moment diagrams are created to provide a visual representation of how the force and moment change along the length of the beam when subjected to a load, as shown in Figure 8.

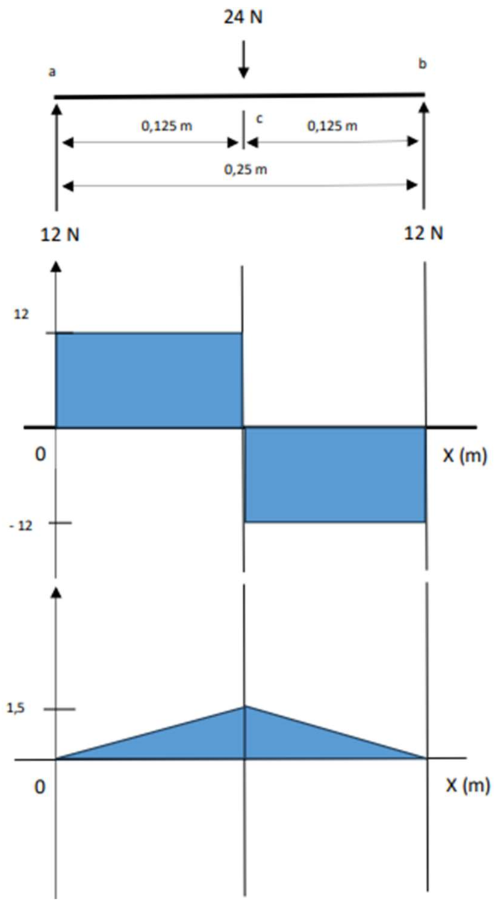

Figure 8. Shear force and bending moment diagrams of the middle support rod.

Moment of Inertia

To obtain the moment of inertia of the middle support rod of the frame, equation (3) can be used.

$$I = I1 + I2 \tag{3}$$

$$= \frac{1}{12} bh^3 + \frac{1}{12} bh^3$$

$$= \frac{1}{12} 0{,}045 \,.\, 0.003^3 + \frac{1}{2} 0{,}042 \,.\, 0.003^3$$

$$= 1{,}9575 \times 10^{-10} m^4$$

Maximum normal stress

To obtain the maximum normal stress on the middle support rod of the frame, equation (4) can be used.

$$\sigma_{max} = \frac{M.C}{1} \tag{4}$$

Description:

σ_{max} = Maximum normal stress ($N/m2$)
M = Bending moment (Nm)
C = Distance of loading point (m)
I = Moment of inertia (m^4)

$$\sigma_{\text{max}} = \frac{M.C}{I}$$

$$= \frac{1{,}5\ N.m\ .0{,}0225\ m}{1{,}9575 \times 10^{-10}\ m^4}$$

$$= 1{,}72414 \times 10^8 N/m^2$$

Safety Factor

To obtain the safety factor on the middle support rod of the frame, equation (5) can be used.

$$sf = \frac{sy}{\sigma_{max}} \tag{5}$$

Description:

sf = Safety factor
sy = Yield strength
σ_{max} = Maximum normal stress (N/m^2)

$$f = \frac{sy}{\sigma_{max}}$$

$$= \frac{250 \times 10^6 \text{ N.m}}{1{,}72414 \times 10^8\ N.m}$$

$$= 1{,}45$$

To see the results of the Maximum Normal Stress and safety factor obtained from the calculations can be viewed in Table 6.

Table 6. Results of maximum normal stress and safety factor calculations.

No	Parts	Maximum Normal Stress σ_{max}	Safety Factor sf
1	Frame	$1{,}72414 \times 10^8$ N/m^2	1,45
2	Shaft	$1{,}07235 \times 10^8$ N/m^2	2,57379

4. CONCLUSION

The air-to-water converter device can be used outdoors as it does not require a household electrical grid but utilizes wind turbines to charge the main battery. The air-to-water converter device is capable of producing 6 ml of water per hour. It is designed based on the second variant where the frame uses ASTM A36 material, the shaft uses aluminum 6061, the turbine blades use galvanized steel, a 12-volt generator, a 12706 thermoelectric type, an outer heatsink of 110 mm × 100 mm, an inner heatsink of 40 mm × 40 mm, a DC 12 V cooling fan (120 mm × 120 mm), an acrylic cooling box, turbine pulleys made of aluminum, generator pulleys made of nylon, energy storage using an accumulator, a solar charge controller (SCC), a plastic funnel, bearings with type UCF 205, and the drive system uses O-ring rubber. The results of theoretical calculations on the frame using ASTM A36 material show a maximum stress of 1.72414×10^8 N/m^2 and a safety factor of 1.45. The results of theoretical calculations on the turbine shaft using aluminum 6061 material yield a maximum stress of 1.07235×10^8 N/m^2 and a safety factor of 2.57379. Based on the theoretical calculation results obtained, it is evident that both the frame and the shaft components meet safety standards.

REFERENCE

[1] W. J. Cosgrove and D. P. Loucks, "Water Resources Research," *JAWRA J. Am. Water Resour. Assoc.*, vol. 5, no. 3, pp. 2–2, 1969, doi: 10.1111/j.1752-1688.1969.tb04897.x.

[2] C. Payus *et al.*, "Impact of extreme drought climate on water security in North Borneo: Case study of Sabah," *Water (Switzerland)*, vol. 12, no. 4, pp. 1–19, 2020, doi: 10.3390/W12041135.

[3] R. Wigati, W. Fathonah, H. B. B. Kuncoro, and H. Mulyono, "Clean water projection of Serang City, Banten Province," *Tek. J. Sains dan Teknol.*, vol. 18, no. 2, p. 111, 2022, doi: 10.36055/tjst.v18i2.16819.

[4] N. Mancosu, R. L. Snyder, G. Kyriakakis, and D. Spano, "Water scarcity and future challenges for food production," *Water (Switzerland)*, vol. 7, no. 3, pp. 975–992, 2015, doi: 10.3390/w7030975.

[5] B. Sivakumar, "Global climate change and its impacts on water resources planning and management: Assessment and challenges," *Stoch. Environ. Res. Risk Assess.*, vol. 25, no. 4, pp. 583–600, 2011, doi: 10.1007/s00477-010-0423-y.

[6] S. Rehana and P. P. Mujumdar, "Climate change induced risk in water quality control problems," *J. Hydrol.*, vol. 444–445, pp. 63–77, 2012, doi: 10.1016/j.jhydrol.2012.03.042.

[7] P. H. Gleick, "Basic water requirements for human activities: Meeting basic needs," *Water Int.*, vol. 21, no. 2, pp. 83–92, 1996, doi: 10.1080/02508069608686494.

[8] A. M. Makarieva, V. G. Gorshkov, D. Sheil, A. D. Nobre, and B. L. Li, "Where do winds come from? A new theory on how water vapor condensation influences atmospheric pressure and dynamics," *Atmos. Chem. Phys.*, vol. 13, no. 2, pp. 1039–1056, 2013, doi: 10.5194/acp-13-1039-2013.

[9] C. R. Kharangate and I. Mudawar, "Review of computational studies on boiling and condensation," *Int. J. Heat Mass Transf.*, vol. 108, pp. 1164–1196, 2017, doi: 10.1016/j.ijheatmasstransfer.2016.12.065.

[10] Razul Harfi, Fadil Gunawan, Veriah Hadi, and Edy Supriyadi, "Perancangan mesin pemotong karet alam dengan menggunakan metode VDI 2221," *JTTM J. Terap. Tek. Mesin*, vol. 3, no. 2, 2022, doi: 10.37373/jttm.v3i2.277.

[11] T. J. Kadhim, A. K. Abbas, and H. J. Kadhim, "Experimental study of atmospheric water collection powered by solar energy using the Peltier effect," *IOP Conf. Ser. Mater. Sci. Eng.*, vol. 671, no. 1, 2020, doi: 10.1088/1757-899X/671/1/012155.

[12] L. W. da Silva and M. Kaviany, "Micro-thermoelectric cooler: Interfacial effects on thermal and electrical transport," *Int. J. Heat Mass Transf.*, vol. 47, no. 10–11, pp. 2417–2435, 2004, doi: 10.1016/j.ijheatmasstransfer.2003.11.024.

[13] E. C. Balke, W. M. Healy, and T. Ullah, "An assessment of efficient water heating options for an all-electric single family residence in a mixed-humid climate," *Energy Build.*, vol. 133, pp. 371–380, 2016, doi: 10.1016/j.enbuild.2016.09.052.

[14] S. A. Feofanov and S. L. Chashchin, "Thermoelectric modular systems based on semiconductor elements of Peltier-Seebeck for vehicles," *J. Phys. Conf. Ser.*, vol. 2061, no. 1, pp. 0–11, 2021, doi: 10.1088/1742-6596/2061/1/012015.

[15] C. J. Atmadja, F. J. Daywin, L. Gozali, C. O. Doaly, and A. P. Irawan, "Improving the capacity of espresso machine using reverse engineering method and VDI 2221 method," *Proc. Int. Conf. Ind. Eng. Oper. Manag.*, pp. 2669–2681, 2021, doi: 10.46254/an11.20210487.

[16] U. S. Ucok, "A Perancangan Pompa Hidram Pada Tabung Udara Dengan Metode VDI 2221,"

TEKNOSAINS J. Sains, Teknol. dan Inform., vol. 7, no. 1, 2020, doi: 10.37373/tekno.v7i1.7.
[17] S. K. Chandrasegaran *et al.*, "The evolution, challenges, and future of knowledge representation in product design systems," *CAD Comput. Aided Des.*, vol. 45, no. 2, pp. 204–228, 2013, doi: 10.1016/j.cad.2012.08.006.